ELSEVIER

Polymer 42 (2001) 6289–6297

polymer

www.elsevier.nl/locate/polymer

# Dynamics of local stiff linear polymers in solutions of high viscosity solvents

Ryszard Szorek

*Textile Institute, Technical University of Łódź, Bielsko-Biała Branch, Willowa 2, 43-309 Bielsko-Biała, Poland*

Received 3 April 2000; received in revised form 8 December 2000; accepted 4 January 2001

**Abstract**

A simple theoretical approach to calculation of dynamic response of local stiff linear polymer chain in semidilute solutions of high viscosity solvents is presented. Using an extended version of the bead–spring hopping model proposed by Jones et al. [J Polym Sci, Phys Ed 1978;16:2215], the dynamic parameters such as: the relaxation time spectra, dynamic shear viscosity $\eta(\omega)/c_p$, complex elastic modulus $G^*(\omega)$ and dielectric constant $\varepsilon(\omega)$ were calculated in the non-free-draining limits. They are shown to be dependent on the polymer concentration $c_p$ and the solvent effective viscosity $\eta_{eff}$. This relationship is compared with experimental data published elsewhere.


*Keywords*: Polymer dynamics theory; Solutions; Low frequency modes

## 1. Introduction

The work presents a theoretical approach to dynamics of linear local stiff polymers in semidilute solutions. It is a new look on the behaviour of vinyl polymers-like polystyrene in solutions of high viscosity solvents such as decaline, aroclor, buthyl phtalate, etc., where at temperatures lying a little above the glass-transition temperature $T_g$ the diffusional arrangement of the polymer chains takes place [1–4].

The experimental data published elsewhere [5,6] show that in non-theta conditions viscoelastic parameters such as the dynamic shear viscosity $\eta(\omega)$ and complex elastic modulus $G^*(\omega)$ of the polymer are quantitatively consistent with those calculated from bead–spring model. The relaxation time spectrum observed at low frequencies in the system considered is shifted due to the finite polymer concentration and the rest of modes behave as if in infinite dilution.

Hess et al. [7] and Muthukumar and Freed [8] on the basis these facts have carried out calculations for dynamics of the polymers in solutions of finite concentration dissolved in ordinary solvents. The results presented in the citied papers show that molecular approach to the problem is a good tool for description of viscoelastic properties of the system. It is confirmed by the results presented in literature [9,10].

We attempt to solve this problem for local stiff linear polymers dissolved in high viscosity solvents using a developed version of the Jones' bead–spring model previously applied to calculation of the single polymer chain dynamics in infinite dilute solutions [11,12]. In addition to this approach the hydrodynamic polymer–polymer interactions are considered now.

All calculations are carried out in the non-free draining limit with respect to intra and interpolymer chain interactions mentioned above. Under these assumptions the dynamic shear viscosity $\eta(\omega)$, complex elastic modulus $G^*(\omega)$ and dielectric constant $\varepsilon(\omega)$ have been calculated.

## 2. Description of the model

The model applied is the hopping model described elsewhere [10–12] concerning now the dynamics of the system of $(N+1)$ beads defined by monomeric units of the polymer immersed in mixture of $(N-1)$ beads familiar systems dispersed in a good solvent. They interact with the related system by friction and hydrodynamic effect. This fact as well as solvent behaviour are incorporated through such elements as the global bead friction coefficient $f$ and hydrodynamic parameters.

So, the related model is visualized, as follows:

A set of an infinite rods $A^{\alpha}_{n-1}, A^{\alpha}_{n}, A^{\alpha}_{n+1}$, etc. fixed in space lies parallel to the $y$ axis, the distance between them in plane $xz$ is, respectively, equal to $a$. Each of these rods is surrounded by $\kappa$ infinite rods $A^{\beta}_{i}$ fixed in their vicinity and parallel to the $y$ axis. They are distributed randomly in the

0032-3861/01/$ - see front matter 
PII: S0032-3861(01)00030-1

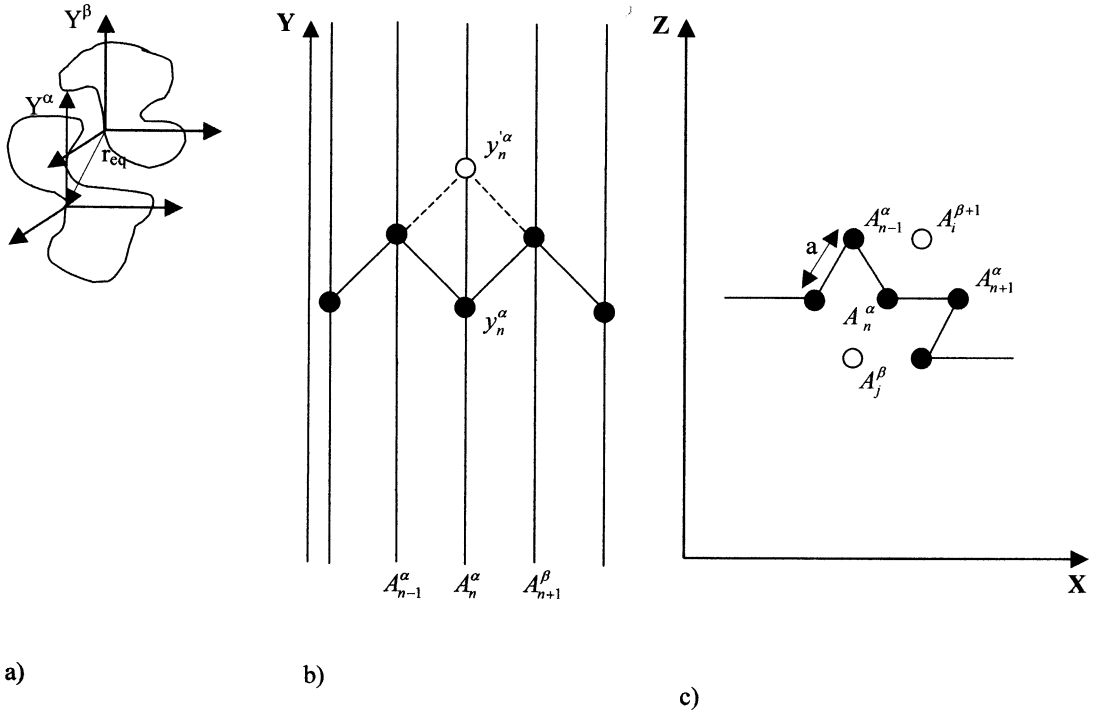


Fig. 1. An illustration of the model: (a) view of the model in space; (b) its view in the *Y* direction; and (c) project onto the *xz* plane.

plane *xz*. The beads are hung on the rods and they are able to slide along each of them. The beads hung on the uniform rods are connected by spring-like segments of the equilibrium length greater than $a$. Moreover, the beads hung on the rods fixed in their vicinity are held at equilibrium distance greater than $r_{eq}$ being equal $r_{eq\geq}a$.

An equlibrium conformation of the beads is a zigzag pattern as is shown in Fig. 1. The distribution of the beads at equilibrium state is governed by one-dimensional random-walk statistics. Also, the angles $A^{\alpha}_{n-1}A^{\alpha}_{n}\,A^{\alpha}_{n+1}$ as well as angles $A^{\beta}_{i-1}\,A^{\beta}_{i}\,A^{\beta}_{i+1}$, etc. are random in plane *xz*.

Because the rods simulate a bond-angle constraints of the polymer chain backbone, the related motion of the beads in the *Y* direction is intended to represent a change of conformation via rotation. Its amplitude is substantially dependent on dynamic rigidity of the $\alpha$ chain being obtained by inter-bead potential defined by double-well function $U(b^{\alpha}_{n})$, where $b^{\alpha}_{n}$ is $b^{\alpha}_{n} = y^{\alpha}_{n} - y^{\alpha}_{n-1}$, and $y^{\alpha}_{n}$ is a coordinate of the $n$th bead.

The system is immersed in a mixture of high viscosity solvent and other systems dispersed with which the beads interact via friction and by hydrodynamic effect. It is obtained by the Stokes friction coefficient $f$ and preaveraged Oseen tensor, respectively. The friction coefficient is expressed now by the effective solvent viscosity $\eta_{\mathrm{eff}}$ being defined as a sum of the solvent shear viscosity $\eta_{\mathrm{s}}$ and viscosity associated with rotation of solvent molecules in the system.

Because the beads are put in motion by thermal fluctuation forces, the dynamics can be described by the system of both equations Langevin and diffusion.

## 3. The diffusion equation formula

Dynamics of the model described above is governed by the following equation

$$\frac{\partial P(y^{1}_{0},\ldots,y^{N}_{N},t)}{\partial t} = -\sum_{\alpha=1}^{N}\sum_{n=1}^{N}\frac{\partial J^{\alpha}_{n}}{\partial y^{\alpha}_{n}}, \tag{1}$$

where

$$J^{\alpha}_{n} = -\frac{1}{f}\left(P\frac{\partial U}{\partial y^{\alpha}_{n}} + kT\frac{\partial P}{\partial y^{\alpha}_{n}}\right) + \sum_{m\neq n} PT^{\alpha}_{nm}\left(\frac{\partial U}{\partial y^{\alpha}_{m}} + kT\frac{\partial \ln P}{\partial y^{\alpha}_{m}}\right) - \sum_{\beta\neq\alpha}\sum_{i} PT^{\alpha\beta}_{ni}\left(\frac{\partial U}{\partial y^{\beta}_{i}} + kT\frac{\partial \ln P}{\partial y^{\beta}_{i}}\right), \tag{2}$$

$$U = \sum_{\alpha=1}^{N}\sum_{n=1}^{N} U(y^{\alpha}_{n} - y^{\alpha}_{n-1}), \tag{3}$$

$$T^{\alpha}_{nm} = \frac{1}{6\pi\eta_{\mathrm{eff}}}\left\langle\frac{1}{y^{\alpha}_{nm}}\right\rangle 1, \qquad T^{\alpha\beta}_{ni} = \frac{1}{6\pi\eta_{\mathrm{eff}}}\left\langle\frac{1}{y^{\alpha\beta}_{ni}}\right\rangle 1. \tag{4}$$

The function $U$ represents the internal energy of the model, $T^{\alpha}_{nm}$ is the hydrodynamic matrix element characteristic for the single $\alpha$ chain, $T^{\alpha\beta}_{ni}$ is the hydrodynamic matrix element

specific for interactions between chains $\alpha$ and $\beta$. The coefficient $f$ is the friction bead coefficient defined now, as

$$f = 6\pi\eta_{\text{eff}}R, \qquad \eta_{\text{eff}} = \eta_{\text{s}} + ckT\tau_{\text{r}}, \tag{5}$$

where $\eta_{\text{s}}$ is the solvent shear viscosity, $R$ is a radius of the bead, $c$ denotes a concentration of solvent molecules rotating in the system, $k$ is the Boltzman constant, $T$ means temperature, $\tau_{\text{r}}$ is the relaxation time of the solvent molecule [13]. Putting the distribution function $P$ given by

$$P = \mathrm{e}^{-U/2kT}\rho_0(\{b_{ni}^{\alpha\beta}\})\rho(\{b_n^{\alpha}\}, t) \tag{6}$$

into Eq. (1) and introducing into it the following variables

$$b_n^{\alpha} = y_n^{\alpha} - y_{n-1}^{\alpha}, \qquad y_n^{\alpha} = \sum_{m=1}^{n} y_m^{\alpha}, \tag{7}$$

we have

$$\frac{f}{kT}\frac{\partial\rho}{\partial t} = \Big[L^0(\{b_n^{\alpha}\}) + L'(\{b_n^{\alpha}, b_{n+1}^{\alpha}\}) + L''(\{b_n^{\alpha}, b_m^{\alpha}\}) + L'''(\{b_n^{\alpha}, b_i^{\beta}\})\Big]\rho, \tag{8}$$

where

$$L^0(\{b_n^{\alpha}\}) = \sum_{\alpha=1}^{N}\sum_{n=1}^{N}\left\{\frac{\partial^2}{\partial b_n^{\alpha 2}} + \frac{1}{2kT}\left[\frac{\partial^2 U}{\partial b_n^{\alpha 2}} - \frac{1}{2kT}\left(\frac{\partial U}{\partial b_n^{\alpha}}\right)^2\right]\right\}, \tag{9}$$

$$L'(\{b_n^{\alpha}, b_{n+1}^{\alpha}\}) = \sum_{\alpha=1}^{N}\sum_{n=1}^{N}\left\{-\frac{\partial^2}{\partial b_n^{\alpha}\partial b_{n+1}^{\alpha}} - \frac{1}{2kT}\left(\frac{\partial^2 U}{\partial b_n^{\alpha}\partial b_{n+1}^{\alpha}} - \frac{1}{2kT}\frac{\partial U}{\partial b_n^{\alpha}}\frac{\partial U}{\partial b_{n+1}^{\alpha}}\right)\right\}, \tag{10}$$

$$L''\left(\left\{b_n^{\alpha}, b_m^{\alpha}\right\}\right) = f\sum_{\alpha=1}^{N}\sum_{m=1}^{N}\sum_{n=1}^{N}\left\{T_{nm}^{\alpha}\left[\frac{\partial^2}{\partial b_n^{\alpha}\partial b_m^{\alpha}} + \frac{1}{2kT}\left(\frac{\partial^2 U}{\partial b_n^{\alpha}\partial b_m^{\alpha}} - \frac{1}{2kT}\frac{\partial U}{\partial b_n^{\alpha}}\frac{\partial U}{\partial b_m^{\alpha}}\right)\right]\right., \tag{11}$$

$$L'''(\{b_n^{\alpha}, b_i^{\beta}\}) = f\sum_{\beta=1}^{N}\sum_{\alpha=1}^{N}\sum_{i=1}^{N}\sum_{n=1}^{N}\left\{T_{ni}^{\alpha\beta}\left[\frac{\partial^2}{\partial b_n^{\alpha}\partial b_i^{\beta}} + \frac{1}{2kT}\left(\frac{\partial^2 U}{\partial b_n^{\alpha}\partial b_i^{\beta}} - \frac{1}{2kT}\frac{\partial U}{\partial b_n^{\alpha}}\frac{\partial U}{\partial b_i^{\beta}}\right)\right]\right.$$
$$\left. - \frac{\partial^2}{\partial b_n^{\alpha}\partial b_{i+1}^{\beta}} + \frac{1}{(2kT)^2}\frac{\partial U}{\partial b_n^{\alpha}}\frac{\partial U}{\partial b_{i+1}^{\beta}}\right\}. \tag{12}$$

Eq. (8) performed above is characteristic for many-particle system dynamics and is similar to that considered in Ref. [11]. Its right-hand side is taken in the next steps as a diffusional operator $L$.

## 4. The configuration interaction method

Eq. (8) is a form similar to that of the Schrodinger equation commonly encountered in quantum mechanics. Its right-hand side is expressed as the sum of the stationary part $L^0(\{b_n^{\alpha}\})$ and three interaction parts: $L'(\{b_n^{\alpha}, b_{n+1}^{\alpha}\})$,, $L''(\{b_n^{\alpha}, b_m^{\alpha}\})$ and $L'''(\{b_n^{\alpha}, b_i^{\beta}\})$. Due to the quantum method the function $\rho$ can be built up as a linear combination of sums constructed from the self-functions $\xi_l(b_n^{\alpha})$ of the operator $L^0(\{b_n^{\alpha}\})$. At boundary conditions introduced for a closed loop polymer chain conformation so that the bead $n = 0$ is identical with the bead $n = N$, the sums mentioned above are defined, as

$$\Psi(\{\mu\}, K) = \frac{1}{N}\sum_{\alpha=1}^{N}\sum_{n=1}^{N}\phi(\{\mu_n^{\alpha}\})\,\mathrm{e}^{\mathrm{i}Kn}, \tag{13}$$

$$\mathbf{K} = \frac{\pi}{N}m, m = \pm 1, \ldots, N,$$

where $\phi(\{\mu_n^{\alpha}\})$ stands for a single product function of $N\xi$'s one for each $b_n^{\alpha}$, in which a certain subset specified by $\{\mu_n^{\alpha}\}$ consists of the functions $\xi_1(b_n^{\alpha})$ for $1 > 0$, describing the state of $b_n^{\alpha}$ excited to l level in the $\alpha$ chain, $\mathbf{K}$ denotes the wave vector specifying the translational symmetry representation of the diffusional operator $L$ to which the state $\Psi(\{\mu\}, K)$ belongs. The function $\phi(\{\mu_n^{\alpha}\})$ may be then written

$$\phi(\{\mu_n^{\alpha}\}) = |\xi(b_n^{\alpha})\rangle \tag{14}$$

and

$$\phi(\{\mu_n^{\alpha}\}) = |\xi_l(b_n^{\alpha})\xi_{l'}(b_{n+m}^{\alpha})\ldots\rangle. \tag{15}$$

The eigenfunctions of the diffusional operator $L$ may be then found by expanding in terms of the $\psi$'s

$$\rho_p(\mathbf{K}) = \sum_{\mu=1}^{\infty} a_{p\mu}(\mathbf{K})\Psi(\{\mu\}, K). \tag{16}$$

The suffix $p$ together with the wave vector $\mathbf{K}$ specifies an eigenfunction of the operator $L$. If $N$ is large, $\mathbf{K}$ approximates to a continuous variable and $p$ specifies a band of eigenvalues $\lambda_{\text{p}}(\mathbf{K})$ corresponding to the eigenfunctions $\rho_{\text{p}}(\mathbf{K})$. At $p = 0$ the $\rho$ function is becoming to be the equilibrium state solution

$$\rho_0 = \mathrm{e}^{-U/2kT}\rho_0(\{b_{ni}^{\alpha\beta}\}) = \left|\xi_0(b_1^1)\ldots\xi(b_N^N)\right\rangle\rho_0(\{b_{ni}^{\alpha\beta}\}). \tag{17}$$

This function fulfils the following equation:

$$L\rho_0 = 0, \tag{18}$$

where $L$ is the diffusion operator expressed by the sum of the operators $L^0(\{b_n^{\alpha}\})$, $L'(\{b_n^{\alpha}, b_{n+1}^{\alpha}\})$, $L''(\{b_n^{\alpha}, b_m^{\alpha}\})$, $L'''(\{b_n^{\alpha}, b_i^{\beta}\})$ and $\rho_0$ is a gaussian expression. $L$'s properties exhibits the equation

$$L\rho = \lambda\rho. \tag{19}$$

Table 1
Sum-rule contributions calculated according to Eq. (21) and the Kramers formula for a simple double-well potential at $\eta_{\text{eff}} = 1.0\eta_s$ ( = 2.5 cP)

| $E_b[kT]$ | $\omega_1$ | $\omega_3$ | $X_{10} = \langle\xi_1\|b\|\xi_0\rangle$ | $X_{30} = \langle\xi_3\|b\|\xi_0\rangle$ | $\omega_1 X_{10}^2$ | $\omega_3 X_{30}^2$ | $\omega_1 X_{10}^2 + \omega_3 X_{30}^2$ |
|---|---|---|---|---|---|---|---|
| 5 | $1.4918 \times 10^{-2}$ | 10.582204 | 0.9834357 | − 0.2268687 | 0.0144279 | 0.5496100 | 0.5640379 |
| 8 | $1.4842 \times 10^{-3}$ | 16.104875 | 0.9992433 | − 0.2433440 | 0.0014820 | 0.9536709 | 0.9551529 |
| 10 | $1.7160 \times 10^{-4}$ | 20.024483 | 0.9998825 | − 0.2223652 | 0.0001716 | 0.9901366 | 0.9903082 |
| 13 | $0.2391 \times 10^{-4}$ | 25.999046 | 0.9999578 | − 0.1958321 | 0.0000239 | 0.9970689 | 0.9970928 |

## 5. Relaxation time spectrum

Relaxation time spectrum of the dynamics observed at double-well potential of the barrier height $E_b$ much more greater than $kT$ is possible to calculate from Eq. (8) by integrating both-its sides using the function $\rho$ constructed from the $\xi_l$ functions defined, as follows

$$\xi_{2l}^{\alpha} = \frac{1}{\sqrt{2}}(\chi_{Al}^{\alpha} + \chi_{Bl}^{\alpha}), \qquad \xi_{2l+1}^{\alpha} = \frac{1}{\sqrt{2}}(\chi_{Al}^{\alpha} - \chi_{Bl}^{\alpha}), \tag{20}$$

where $\chi_{A1}^{\alpha}, \chi_{B1}^{\alpha}$ are the eigenfunctions of the harmonic oscillator type centered at points A and B and completely separated in space. The functions $\xi_{2l}^{\alpha}, \xi_{2l+1}^{\alpha}$ are, respectively, even and odd eigenfunctions of the $L^0$ operator describing at $l = 0$ the degenerated state $\omega_1 = \omega_0 = 0$. However, at $l > 0$ they are describing states of the $b_n^{\alpha}$ segment in damped oscillations within each well. This fact corresponds to states of the model due to the motion.

As $E_b$ is reduced, the degeneracy effect disappears and the states $\omega_0$, $\omega_1$ are lifted. In consequence of the $b_n^{\alpha}$ segment escapes over an energy barrier $E_b \gg kT$ from position A to B. The state $\omega_0$ is a ground state of the system described by the symmetric functions $\xi_0^{\alpha}$. On the other hand, the state of eigenvalue $\omega_1$ is excited state of the system described by antisymmetric functions $\xi_1^{\alpha}$ representing redistribution of bead density between positions A and B. The bead relaxes by diffusion over an energy barrier $E_b$ and the value $\omega_1$ corresponding to frequency of the bead hopping is obtained by the Kramers formula [14]. Independently to this relaxation the bead is governed by librational modes of the frequency $\omega_3 \approx \omega_2$. All frequencies are subjected to the sum rule for the oscillator strength written in general form, as

$$\sum_{l=1}^{\infty} \omega_l \langle\xi_l|b|\xi_0\rangle^2 = 1. \tag{21}$$

Behaviour of the latter formula is illustrated by the data presented in Table 1. The data have been calculated for a simple double-well potential of an energy barrier height $E_b$ varied from 5 to 13$kT$.

Application of formula (21) to Eqs. (8) and (9) leads to the following equation

$$\left\langle \Psi^*(l',K) \middle| \sum_{\alpha=1}^{N} \sum_{n=1}^{N} L^0(b_n^{\alpha}) \middle| \Psi(l,K) \right\rangle = -\omega_l \delta n n' \delta\alpha\beta\delta l l', \tag{22}$$

where the functions $\Psi(l, K)$ are expressed now throughout functions (20) put for the functions $\phi$ in Eq. (13) and $\omega_1$ is an angle self-frequency of the model at $l$th excitation. The same approach applied to calculation of the matrix elements $\langle\Psi^*(l', K)|L'(\{\{b_n^{\alpha}, b_{n+1}^{\alpha}\}\}|\Psi(l, K)\rangle$ gives

$$\begin{aligned}
&\left\langle \Psi^*(l',K) \middle| \sum_{\alpha=1}^{N} \sum_{n=1}^{N} L'(b_n^{\alpha}, b_{n+1}^{\alpha}) \middle| \Psi(l,K) \right\rangle \\
&= \frac{2}{N^2} \sum_{\alpha=1}^{N} \sum_{n=1}^{N} \left( \left\langle \xi_{l'}(b_n^{\alpha}) \middle| \frac{\partial}{\partial b_n^{\alpha}} \middle| \xi_0(b_n^{\alpha}) \right\rangle \right. \\
&\quad \times \left\langle \xi_l(b_{n+1}^{\alpha}) \middle| \frac{\partial}{\partial b_{n+1}^{\alpha}} \middle| \xi_0(b_{n+1}^{\alpha}) \right\rangle \\
&\quad \left. + \left\langle \xi_{l'}(b_{n+1}^{\alpha}) \middle| \frac{\partial}{\partial b_{n+1}^{\alpha}} \middle| \xi_0(b_{n+1}^{\alpha}) \right\rangle \right),
\end{aligned} \tag{23}$$

$$\begin{aligned}
&\left\langle \xi_l(b_n^{\alpha}) \middle| \frac{\partial}{\partial b_n^{\alpha}} \middle| \xi_0(b_n^{\alpha}) \right\rangle \cos K \\
&= \frac{2}{N^2} \sum_{\alpha=1}^{N} \sum_{n=1}^{N} \omega_{l'} \omega_l \xi_{l'}(b_n^{\alpha}) |b_n^{\alpha}| \xi_0^{\alpha} \left( \left\langle \xi_{l'}(b_n^{\alpha}) b_n^{\alpha} | \xi_0^{\alpha} \right\rangle \right. \\
&\quad \times \left\langle \xi_l(b_{n+1}^{\alpha}) | b_{n+1}^{\alpha} | \xi_0(b_{n+1}^{\alpha}) \right\rangle \\
&\quad \left. + \left\langle \xi_{l'}(b_{n+1}^{\alpha}) | b_{n+1}^{\alpha} | \xi_0(b_{n+1}^{\alpha}) \right\rangle \left\langle \xi_l(b_n^{\alpha}) | b_n^{\alpha} | \xi_0(b_n^{\alpha}) \right\rangle \right) \cos K \\
&= \omega_{l'} \omega_l \left\langle \xi_{l'} | b | \xi_0 \right\rangle \left\langle \xi_l | b | \xi_0 \right\rangle \cos K,
\end{aligned}$$

where the following relationship

$$\left\langle \xi_l | [L^0, b_n^{\alpha}] | \xi_0 \right\rangle = 2 \langle \xi_l | \frac{\partial}{\partial b_n^{\alpha}} | \xi_0 \rangle = \omega_l \langle \xi_l | b_n^{\alpha} | \xi_0 \rangle \tag{24}$$

has been used. In order, two next matrix elements $\langle\Psi^*(l', K)|L''|Y(l, K)\rangle$ and $\langle\Psi^*(l', K)|L'''|\Psi(l, K)\rangle$ calculated according to the method described above are expressed, as follows:

$$\begin{aligned}
&\langle \Psi^*(l',K) | \sum_{\alpha=1}^{N} \sum_{m=1}^{N} \sum_{n=1}^{N} L''(b_n^{\alpha}, b_m^{\alpha}) \Psi(l,K) \rangle \\
&= -\omega_{l'} \omega_l h I \langle \xi_{l'} | b | \xi_0 \rangle \langle \xi_l | b | \xi_0 \rangle (1 - \cos K),
\end{aligned} \tag{25}$$

Table 2
Influence of the hydrodynamic interaction on the band $\lambda_3^H(K)$ calculated from formula (31) for $N = 1000$ and energy barrier height $E_b = 13kT$ at several values of the polymer swelling parameter and polymer concentrantion $c_p$

| $\lambda_3^H(K) \times 10^3$ | | | | | | |
|---|---|---|---|---|---|---|
| $K \times 10^3$ | $c_p = 0, \varepsilon = 0$ | $c_p = 0.5, \varepsilon = 0$ | $c_p = 1.0, \varepsilon = 0$ | $c_p = 0, \varepsilon = 0.2$ | $c_p = 0.5, \varepsilon = 0.2$ | $c_p = 1.0, \varepsilon = 0.2$ |
| 0.0 | 0.0 | 0.0 | 0.0 | 0.0 | 0.0 | 0.0 |
| 3.141 | 16.750 | 25.442 | 32.743 | 13.381 | 19.313 | 24.845 |
| 6.283 | 87.313 | 132.530 | 170.614 | 71.170 | 102.798 | 132.301 |
| 9.425 | 249.355 | 378.662 | 487.569 | 200.834 | 290.226 | 373.614 |
| 12.566 | 500.472 | 760.147 | 978.854 | 406.042 | 587.908 | 755.627 |
| 15.708 | 887.147 | 1347.692 | 1735.580 | 715.828 | 1034.882 | 1332.507 |
| 18.849 | 1383.530 | 2101.976 | 2707.080 | 1120.860 | 1620.638 | 2086.849 |

and

$$\langle \Psi^*(l', K)| \sum_{\beta=1}^{N} \sum_{\alpha=1}^{N} \sum_{i=1}^{N} \sum_{n=1}^{N} L'''(b_n^\alpha, b_i^\beta) \Psi(l, K)\rangle$$

$$= -c_p V \omega_{l'} \omega_l h I \langle \xi_{l'}|b|\xi_0\rangle\langle \xi_l|b|\xi_0\rangle(1 - \cos K), \quad (26)$$

where $c_p$ means the polymer concentration, $V$ is the volume unit element and $h$ is the hydrodynamic parameter. Its value is calculated from the formula derived according to the Kikwood–Riseman theory [11,15] with respect to Ptisyn–Eisner [16] and Muthukumar–Freed [8] approximations. It is expressed by

$$h = \frac{2^{\varepsilon/2} N f}{\sqrt{12\pi^3} b \eta_{\text{eff}} N^{(1+\varepsilon)/2}}, \quad (27)$$

$$I = \left(\frac{\pi\nu}{2}\right)^{(1+\varepsilon)/2} \int_0^Y \frac{\cos(t)}{t^{(1+\varepsilon)/2}} \mathrm{d}t,$$
$$I' = \left(\frac{\pi\nu}{2}\right)^{(1+\varepsilon)/2} \int_0^Y \frac{\cos(t)}{(t^{(1+\varepsilon)} + t' N^{-\varepsilon})^{1/2}} \mathrm{d}t\, \mathrm{d}t', \quad (28)$$

where $I$ and $I'$ are the Fresnel integrals. The sum of the formulae (22), (23), (25) and (26) corresponds to the integral of right-hand side of the diffusion Eq. (8). Its diagonal elements are equal to the relaxation time spectrum $\lambda_1(K)$

$$\lambda_l^H(K) = \omega_l\{1 + (I + c_p V I')h\omega_l \langle \xi_l|b|\xi_0\rangle^2 - h[1 + (I + c_p V I')]\omega_l \langle \xi_l|b|\xi_0\rangle^2 \cos K\} \quad (29)$$

characteristic for dynamic excitation of the model to $l$ level. In this case two bands: diffusional $\lambda_1^H(K)$ and librational $\lambda_3^H(K)$ are considered. The first is associated with hopping of the beads over an energy barrier $E_b$ and the second with their liberation around equilibrium position. Its nature has been previously described in detail [11]. At $h$ equal to zero both bands become the form characteristic for the free-draining case and at $E_b \geq 10kT$ they are, respectively, narrow

$$\lambda_1 = \omega_1 \quad (30)$$

and wide

$$\lambda_3^H(K) = \omega_3[1 + h(I + c_p V I')(1 - \cos K)]. \quad (31)$$

For $N \geq 1000$ the integral $I'$ may be approximated to the integral $I$ and the last expression becomes simpler. This fact closely corresponds to the model. It is confirmed by the data presented in Tables 1 and 2.

As, it is seen the band $\lambda_3^H(K)$ quickly achieves higher levels with increase of $K$ values. This effect disappears at $K$ values lying above the point $K_0$. In this range $\lambda_3^H(K)$ increases slowly to higher levels involving coupling effect between neighbour excited states [17]. It is not considered in this work. The dynamics is calculated for $K$ lying within the range: $0 < K < K_0$ and $c_p < c_p^{kr}$, where $c_p^{kr}$ is the polymer concentration at which hopping effect in the polymer chain is not possible to occur.

Under these conditions a contribution of the interpolymer excluded volume effect to the dynamics is becoming to be small and is neglected in the calculations.

## 6. Calculation of the dynamic shear viscosity $\eta(\omega)$

The calculations of the viscosity $\eta(\omega)$ are carried out according to the Zimm method described in Ref. [18] by the use of the standard perturbation theory. Due to this fact, the master diffusion equation is considered now in the perturbational form being obtained from Eq. (8) by introducing into it the following perturbation

$$v_y^0 = g_0 \, \mathrm{e}^{\mathrm{i}\omega t} \sum_{\alpha=1}^{N} \sum_{n=1}^{N} x_n^\alpha, \quad (32)$$

where $v_y^0$ is the solvent velocity, $g_0$ is an amplitude of the solvent velocity gradient $g$, $\omega$ denotes angle frequency of the perturbation, $t$ means time and $X_n^\alpha$ is the coordinate of the nth bead in the $\alpha$ chain.

As the result of the mathematical operation carried out we

Table 3
Contribution of the viscosity $\eta_1(\omega)/c_p$ and $\eta_3(\omega)/c_p$ into the dynamic viscosity of the sytem $\eta(\omega)/c_p$ calculated according to Eq. (39) at $\varepsilon = 0$ for $N = 1000$ ($M = 10^6$), energy barrier $E_b = 13kT$ and several values of the polymer concentration $c_p$

| Log($\omega$) | $c_p = 0$ | | | $c_p = 0.5$ | | | $c_p = 1.0$ | | |
|---|---|---|---|---|---|---|---|---|---|
| | $\eta_1(\omega)/c_p \times 10^{10}$ | $\eta_3(\omega)/c_p$ | $\eta(\omega)/c_p$ | $\eta_1(\omega)/c_p \times 10^{10}$ | $\eta_3(\omega)/c_p$ | $\eta\ (\omega)/c_p$ | $\eta_1(\omega)/c_p \times 10^{10}$ | $\eta_3(\omega)/c_p$ | $\eta\ (\omega)/c_p$ |
| −7.0 | 57.440 | 1.199 | 1.199 | 57.440 | 0.804 | 0.804 | 57.440 | 0.604 | 0.604 |
| −6.5 | 57.431 | 1.199 | 1.199 | 57.430 | 0.804 | 0.804 | 57.430 | 0.604 | 0.604 |
| −6.0 | 57.341 | 1.199 | 1.199 | 57.333 | 0.804 | 0.804 | 57.326 | 0.604 | 0.604 |
| −5.5 | 56.454 | 1.199 | 1.199 | 56.383 | 0.804 | 0.804 | 56.309 | 0.604 | 0.604 |
| −5.0 | 48.889 | 1.199 | 1.199 | 48.362 | 0.804 | 0.804 | 47.827 | 0.604 | 0.604 |
| −4.5 | 20.894 | 1.199 | 1.199 | 19.963 | 0.804 | 0.804 | 19.082 | 0.64 | 0.604 |
| −4.0 | 3.106 | 1.199 | 1.199 | 2.905 | 0.804 | 0.804 | 2.722 | 0.604 | 0.604 |
| −3.5 | 0.326 | 1.197 | 1.197 | 0.304 | 0.803 | 0.803 | 0.284 | 0.604 | 0.604 |
| −3.0 | 0.033 | 1.182 | 1.182 | 0.030 | 0.798 | 0.798 | 0.028 | 0.602 | 0.602 |

have

$$\frac{f}{kT}\frac{\partial\rho}{\partial t} = \Bigg[\sum_{\alpha=1}^{N}\sum_{n=1}^{N}\frac{fg}{kT}(x_n^\alpha - x_{n-1}^\alpha)\frac{\partial}{\partial b_n^\alpha} + L^0(\{b_n^\alpha\}) + L'(\{b_n^\alpha, b_{n+1}^\alpha\}) + L''(\{b_n^\alpha, b_m^\alpha\}) + L'''(\{b_n^\alpha, b_i^\beta\})\Bigg]\rho. \tag{33}$$

The function $\rho$ is defined now, as follows

$$\rho = \rho_0 + \frac{fg}{kT}\sum_K\sum_l \frac{\langle\Psi(1,K)|\sum_{\alpha=1}^{N}\sum_{n=1}^{N}(x_n^\alpha - x_{n-1}^\alpha)|\rho_0\rangle}{\lambda_l^H(K) + i\omega}\Psi(l,K). \tag{34}$$

Its application to the definition of the shear viscosity given by

$$\frac{\eta(\omega)}{c_p} = -\frac{N_a}{Mg\eta_s}\left\langle\sum_{\alpha=1}^{N}\sum_{n=1}^{N}F_{y_n^\alpha}x_n^\alpha\right\rangle = -\frac{N_a}{Mg\eta_s}\sum_{\alpha=1}^{N}\sum_{n=1}^{N}\left\langle-\left(\frac{\partial U}{\partial y_n^\alpha} + kT\frac{\partial \ln P}{\partial y_n^\alpha}\right)\right\rangle \tag{35}$$

leads to the following expression

$$\frac{\eta(\omega)}{c_p} = -\frac{N_a}{Mg\eta_s}\sum_{\alpha=1}^{N}\sum_{n=1}^{N}\left\langle(x_n^\alpha - x_{n-1}^\alpha)\left(\frac{\partial U}{\partial b_n^\alpha} + kT\frac{\partial \ln P}{\partial b_n^\alpha}\right)\right\rangle = \frac{N_a f}{Mg\eta_s}\sum_K\sum_l\frac{\langle\Psi(1,K)|\sum_{\alpha=1}^{N}\sum_{n=1}^{N}(x_n^\alpha - x_{n-1}^\alpha)\frac{\partial}{\partial b_n^\alpha}|\rho_0\rangle^2}{\lambda_l^H(K) + i\omega}, \tag{36}$$

where $N_a$ is the Avogadro's number and $M$ denotes molecular weight of the polymer. After integration the last expression takes the following form

$$\frac{\eta(\omega)}{c_p} = \frac{N_a f\left\langle b_0^2\right\rangle}{6M\eta_s}\sum_K\sum_l\frac{\omega_l^2|\langle\xi_l|b|\xi_0\rangle|^2}{\lambda_l^H(K) + i\omega}, \tag{37}$$

where

$$\left\langle(x_n^\alpha - x_{n-1}^\alpha)(x_{n'}^\alpha - x_{n'-1}^\alpha)\right\rangle = \frac{1}{3}\left\langle b_0^2\right\rangle. \tag{38}$$

At conditions assumed above formula (37) becomes

$$\frac{\eta(\omega)}{c_p} = \frac{N_a f\left\langle b_0^2\right\rangle}{6M\eta_s}\sum_K\left(\frac{\omega_1^2|\langle\xi_1|b|\xi_0\rangle^2}{\lambda_1 + i\omega} + \frac{\omega_3^2|\langle\xi_3|b|\xi_0\rangle^2}{\lambda_3^H(K) + i\omega}\right) = \frac{\eta_1(\omega)}{c_p} + \frac{\eta_3(\omega)}{c_p}. \tag{39}$$

Its behaviour in function of the frequency $\omega$ exhibit the data collected in Table 3 and the curves shown in Fig. 2.

As it is seen, the component $\eta_1(\omega)/c_p$ introduces unexpectively small contribution to the viscosity $\eta(\omega)/c_p$. Its frequency-dependence typical for single bead relaxation phenomenon is not dependent on the polymer concentration $c_p$ and does not apparently contribute to the dispersion curves presented in Fig. 2. On the other hand, the second component appears dominant and dependent on the polymer concentration $c_p$. Its character is the Rouse–Zimm-like for enough long polymer chain dynamics. It is reflected in shape and position in the coordinate system of the discussed dispersion curves. They are influenced by the polymer concentration $c_p$ preserving Rouse-like character within the frequency range: $10^{-2}$–$10^2$ Hz. All curves presented above are frequency-dependent falling to zero with increase of log $\omega$ to 2.

## 7. The dynamic elastic modulus $G^*(\omega)$

The complex elastic modulus $G^*(\omega)$ is the second parameter characterizing viscoelastic properties of the polymer [19]. Its value is determined by dynamic elasticity of the polymer and can be calculated from the following relationship

$$G^*(\omega) = G'(\omega) + iG''(\omega) = i\omega\eta_s[1 + \eta(\omega)/c_p], \tag{40}$$

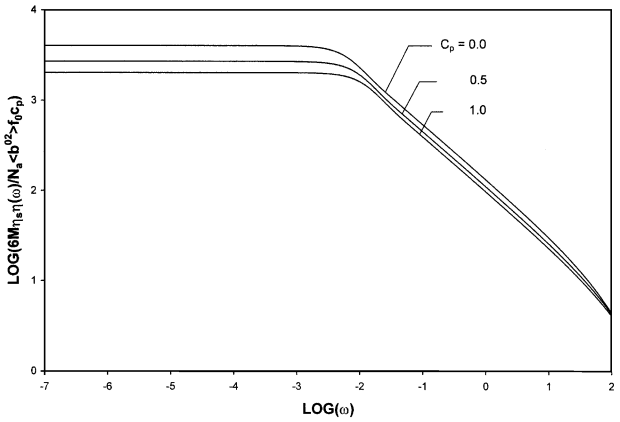


Fig. 2. Plot of $\log(6M\eta(\omega)\eta_s/N_a f_0\langle b_0^2\rangle c_p)$ vs. $\log\omega$ prepared for $N = 1000$ and several values of the polymer concentration $c_p$ equal to 0, 0.5, 1.0. The curves shown represent the model calculations carried out according to Eqs. (39) and (5) with $\eta_s = 2.5$ cP.

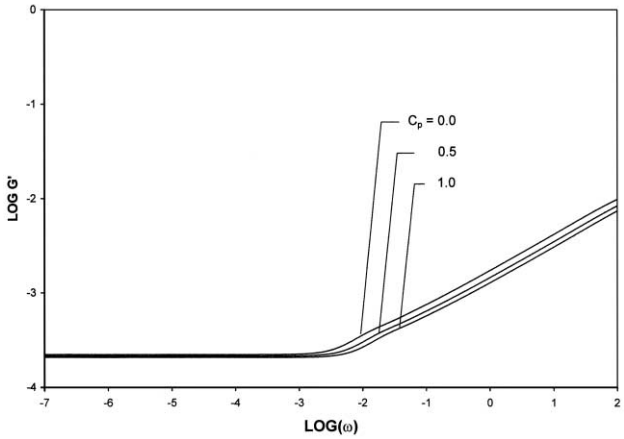


Fig. 3. Logarithm of the storage elastic modulus $\log G'$ in function of $\log\omega$ for $N = 1000$, $c_p$ equal to 0, 0.5, 1.0 and $\eta_s = 2.5$ cP.

where $\eta(\omega)$ is the dynamic shear viscosity given by Eq. (39), $G'(\omega)$ denotes the storage elastic modulus and $G''(\omega)$ is the loss elastic modulus. The curves shown in Figs. (3) and (4) exhibit behaviour of both modulae calculated for the model according to Eq. (39). They are plotted as $\log G'(\omega)$ and $\log(G'' - \omega\eta_s)$ vs. $\log\omega$.

The plots presented below show that frequency-dependence of both modulae $G'$ and $G''$ are sensitive to change of the polymer concentration $c_p$ within the range characteristic for librational modes. This fact as well as relatively slow increase of the mentioned modulae to higher level in this frequency range exhibits the Rouse–Zimm character of the model. It is corresponding to experimental data published elsewhere [20].

## 8. The dielectric constant $\varepsilon(\omega)$

The effect of electric field interaction with the system is calculated according to the method used above starting from the perturbation [11,13]

$$U' = U - q\sum_{\alpha=1}^{N}\sum_{n=1}^{N} E_{y_n^\alpha} y_n^\alpha, \tag{41}$$

where $q$ is an elementary electric charge and $E_y$ is the local electric field intensity.

Introduction of the potential $U'$ into Eq. (8) leads to the following equation

$$\frac{f}{kT}\frac{\partial\rho}{\partial t} = [L^0(\{b_n^\alpha\}) + L'(\{b_n^\alpha, b_{n+1}^\alpha\}) + L''(\{b_n^\alpha, b_m^\alpha\}) + L'''(\{b_n^\alpha, b_i^\beta\}) + L^{\mathrm{IV}}(\{b_n^\alpha, b_m^\beta\}) + L^{\mathrm{V}}(\{b_n^\alpha, b_i^\beta\})]\rho, \tag{42}$$

where $L^0(\{b_n^\alpha\}), L'(b_n^\alpha, b_{n+1}^\alpha), L''(\{b_n^\alpha, b_m^\alpha\})$ and $L'''(\{b_n^\alpha, b_i^\beta\})$ are the operators, respectively, obtained by Eqs. (9)–(12). In turn, the operators

$$L^{\mathrm{IV}}(\{b_n^\alpha, b_m^\alpha\})$$

and

$$L^{\mathrm{V}}(\{b_n^\alpha, b_i^\beta\})$$

are given by

$$L^{\mathrm{IV}}(\{b_n^\alpha, b_m^\alpha\}) = \frac{qE}{3kT}\sum_{\alpha=1}^{N}\sum_{m=1}^{N}\sum_{n=1}^{N} H_{nm}^\alpha\left[\frac{1}{kT}\left(\frac{\partial U}{\partial b_m^\alpha}\right) - \frac{\partial}{\partial b_m^\alpha}\right], \tag{43}$$

$$L^{\mathrm{V}}(\{b_n^\alpha, b_i^\beta\}) = \frac{qE}{3kT}\sum_{\beta=1}^{N}\sum_{\alpha=1}^{N}\sum_{i=1}^{N}\sum_{n=1}^{N} H_{ni}^{\alpha\beta}\left[\frac{1}{kT}\left(\frac{\partial U}{\partial b_i^\beta}\right) - \frac{\partial}{\partial b_i^\beta}\right], \tag{44}$$

where $H_{nm}^\alpha$ and $H_{ni}^{\alpha\beta}$ are hydrodynamic matrix elements written as

$$H_{nm}^\alpha = \delta_{nm} + fT_{nm}^\alpha; H_{ni}^{\alpha\beta} = \delta_{nm}^{\alpha\beta} + fT_{nm}^{\alpha\beta} \tag{45}$$

and $E$ is the intensity of the electric field applied to the system

$$E = E_0\,\mathrm{e}^{\mathrm{i}\omega t}. \tag{46}$$

Due to these facts, the function $\rho$ can be expressed by

$$\rho = \rho_0 + \frac{qE}{3kT}\sum_K\sum_l \frac{\left\langle\Psi(l,K)|L^{\mathrm{IV}} + L^{\mathrm{V}}|\rho_0\right\rangle}{\lambda_l^{\mathrm{H}}(K) + \mathrm{i}\omega}\Psi(l,K). \tag{47}$$

Application of this function to the definition of the electric polarization

$$p = \frac{1}{E}\sum_{\alpha=1}^{N}\sum_{n=1}^{N}\langle q b_n^\alpha\rangle \tag{48}$$

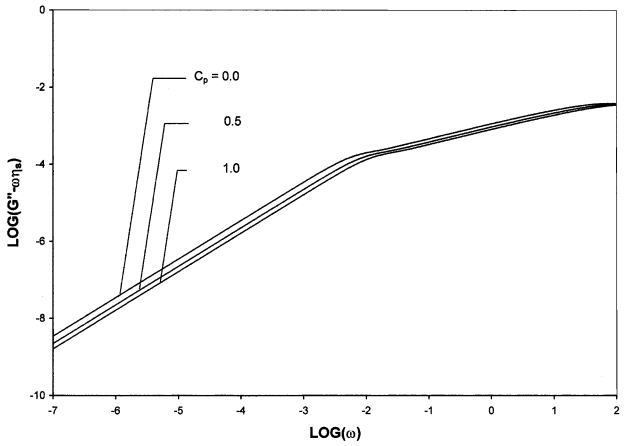


Fig. 4. Logarithm of the loss elastic modulus $\log(G'' - \omega\eta_s)$ plotted vs. log $\omega$. The curves presented were calculated for the same parameters as in Fig. 3.

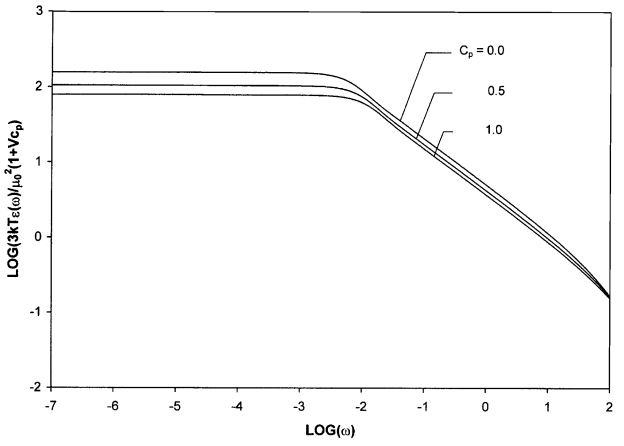


Fig. 5. Variation of log $[3kT\epsilon(\omega)/\mu_0^2(1 + Vc_p)]$ as a function of log $\omega$ obtained according to Eq. (51) for $c_p$ equal to 0, 0.5, 1.0; $N = 1000$ and $\eta_s = 2.5$ cP.

gives

$$p(\omega) = \frac{q^2}{3kT}\sum_K\sum_l \frac{\left\langle \Psi(l,K)|L^{IV} + L^{V}|\rho_0\right\rangle}{\lambda_l^H(K) + i\omega} \times\langle\Psi(l,K)|\sum_{\alpha=1}^{N}\sum_{n=1}^{N} b_n^{\alpha}|\rho_0\rangle = \frac{q^2}{3kT}\sum_K\sum_l \frac{(1 + Vc_p)\omega_l|\langle\xi_1|b|\xi_0\rangle|^2}{\lambda_l^H(K) + i\omega}, \quad (49)$$

where the matrix elements $\left\langle \Psi^*(l,K)|H|\Psi(l,K)\right\rangle$ equal to 1 has been used. At conditions assumed above the last formula becomes

$$p(\omega) = \frac{\mu_0^2}{3kT}\sum_K\left[\frac{(1 + Vc_p)\omega_1\left|\left\langle \xi_1|b|\xi_0\right\rangle\right|^2}{\lambda_1 + i\omega} + \frac{(1 + Vc_p)\omega_3\left|\left\langle \xi_3|b|\xi_0\right\rangle\right|^2}{\lambda_3^H(K) + i\omega}\right], \quad (50)$$

where $\mu_0$ is the dipole per unit length.

Then, the dielectric constant $\epsilon(\omega)$ is given by

$$\epsilon(\omega) = 1 + p(\omega) = \frac{\mu_0^2(1 + Vc_p)}{3kT}\sum_K\left(\frac{\omega_1|\langle\xi_1|b|\xi_0\rangle|^2}{\lambda_1 + i\omega} + \frac{\omega_3|\langle\xi_3|b|\xi_0\rangle|^2}{\lambda_3^H(K) + i\omega}\right). \quad (51)$$

The curves shown in Fig. 5 are similar to those demonstrated in Fig. 2 for the dynamic viscosity $\eta\ (\omega)/c_p$. They were prepared according to the data received from Eq. (51) at the same conditions as those applied to calculation of the viscosity. Due to this fact, the considered dipole relaxation seems to be closely similar to the relaxation of the viscoelastic parameters discussed above. This fact confirm the available experimental data [21].

## 9. Conclusions

A theoretical approach to the dynamics of local stiff vinyl polymers-like polystyrene in semidilute solutions of high viscosity solvents at finite concentration is presented in this work. The calculations for the relaxation spectrum $\lambda_1^H$, dynamic shear viscosity $\eta(\omega)$, complex elastic modulus $G^*(\omega)$ and dielectric constant $\epsilon(\omega)$ were carried out for the hopping model proposed by Jones et al. [10] with respect to intra and interpolymer interactions.

The results of these calculations show that the vinyl polymers in high viscosity solvents such as decaline, aroclors, etc. at concentration $c_p > c_p^{kr}$ are able to change the conformation via rotation and librational motions around equilibrium position. The first process is obtained by the narrow band $\lambda_1$ characteristic for the single-bead-Debye relaxation and the second process by the wide band $\lambda_3^H(K)$ specific for the Rouse–Zimm relaxation. Both processes are diffusional and each other independent. They are influenced by the effective solvent viscosity $\eta_{eff}$. The second process represented by the band $\lambda_3^H(K)$ is described for the wave vector **K** lying within the range $0 < K < K_0$.

Position and shape of the band $\lambda_3^H(K)$ is determined by the self-bead-frequency $\omega_3$, the nearest-neighbour-interaction specified by the wave vector **K**, intra and interpolymer interactions. Due to this fact, this band is shifted into higher frequencies in relation to position of its familiar form calculated in the free-draining limits. The polymer concentration $c_p$ introduces significant contribution to this effect. It is reflected in behaviour of the viscoelastic parameters and dielectric constant calculated for the model (Figs. 2–5).

The dynamic shear viscosity $\eta\ (\omega)/c_p$ drops down to

lower level with increase of the polymer concentration and falls to zero with increase of the frequency $\omega$ up to 100 Hz. The same behaviour is observed for the dielectric constant $\epsilon(\omega)$.

The complex elastic modulus $G^*(\omega)$ represented by the storage $G'(\omega)$ and loss elastic modulus $G''(\omega)$ calculated for the model appears less sensitive to change of the polymer concentration $c_p$ than the dynamic viscosity and dielectric constant. However, they also decrease to lower level with increase of the polymer concentration.

All discussed quantities are unexpectedly mildly sensitive to the single-bead relaxation process.

## References

[1] Helfand E. J Chem Phys 1971;54:4651.
[2] Baily RT, North AM, Pethrick RA. Molecular motion in high polymers. Oxford: Clarendon Press, 1981.
[3] Binder K, Paul W. J Polym Sci, Part B: Polym Phys 1997;35:1.
[4] Gonzalez Mac Dowell L, Muller M, Vega C, Binder K. J Chem Phys 2000;113:419.
[5] Fredrickson GH, Helfand E. J Chem Phys 1990;93:2048.
[6] Johnson RM, Schrag JL, Ferry JD. Polym J 1970;1:742.
[7] Hess W, Jilge W, Klein R. J Polym Sci, Phys Ed 1981;19:849.
[8] Muthukumar M, Freed KF. Macromolecules 1978;11:843.
[9] Freed K. In: Croxton CA, editor. Progress in liquid physics. New York: Wiley, 1978.
[10] Jones DA, Lopez de Haro M, Pugh D. J Polym Sci, Phys Ed 1978;16:2215.
[11] Szorek R. Chem Phys 1999;241:83.
[12] Szorek R. J Chem Phys 1985;83:1421.
[13] Harnau L, Winkler RG, Reineker P. J Chem Phys 1995;102:7750.
[14] Kramers HA. Physica 1940;7(4):284.
[15] Kirkwood JG, Riseman J. J Chem Phys 1948;16:565.
[16] Ptisyn OB, Eisner YuE. Zh Tekhn Fiz 1958;32:2464.
[17] Szorek R. Chem Phys 1999;246:335.
[18] Zimm BH. J Chem Phys 1956;24:269.
[19] Adler RS, Freed KF. J Chem Phys 1980;72:2032.
[20] Schmieder K, Wolf K. Kolloid Z 1953;134:149.
[21] Kästner S, Schlosser E, Pohl G. Kolloid Z 1963;192:21.